Carbohydrate Research 344 (2009) 1753–1757

Contents lists available at ScienceDirect

Carbohydrate Research

journal homepage: www.elsevier.com/locate/carres

The crystal structure of a family GH25 lysozyme from *Bacillus anthracis* implies a neighboring-group catalytic mechanism with retention of anomeric configuration

Carlos Martinez-Fleites, Justyna E. Korczynska, Gideon J. Davies, Matthew J. Cope, Johan P. Turkenburg, Edward J. Taylor *

Structural Biology Laboratory, Department of Chemistry, The University of York, YO10 5YW, United Kingdom

ARTICLE INFO

Article history:
Received 5 March 2009
Received in revised form 27 May 2009
Accepted 1 June 2009
Available online 6 June 2009

Keywords:
Lysozyme
Autolysin
Peptidoglycan cleavage
Anthrax
Hexosaminidase

ABSTRACT

Lysozymes are found in many of the sequence-based families of glycoside hydrolases (www.cazy.org) where they show considerable structural and mechanistic diversity. Lysozymes from glycoside hydrolase family GH25 adopt a $(\alpha/\beta)_5(\beta)_3$-barrel-like fold with a proposal in the literature that these enzymes act with inversion of anomeric configuration; the lack of a suitable substrate, however, means that no group has successfully demonstrated the configuration of the product. Here we report the 3-D structure of the GH25 enzyme from *Bacillus anthracis* at 1.4 Å resolution. We show that the active center is extremely similar to those from glycoside hydrolase families GH18, GH20, GH56, GH84, and GH85 implying that, in the absence of evidence to the contrary, GH25 enzymes also act with net retention of anomeric configuration using the neighboring-group catalytic mechanism that is common to this 'super-family' of enzymes.

1. Introduction

Lysozyme is a generic term given to describe hydrolytic enzymes which cleave the β-1,4-glycosidic bond between *N*-acetylmuramic acid (NAM) and *N*-acetylglucosamine (NAG) and in the carbohydrate backbone (**1**) of bacterial peptidoglycan.

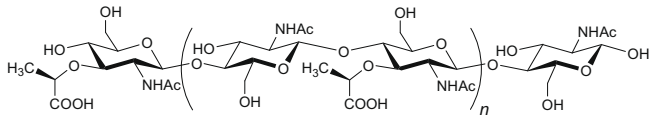

1

There is an increasing interest in harnessing the lytic properties of these enzymes as antimicrobial agents due to their exquisite efficiency[1] and specificity against medical relevant pathogens such as *Streptococcus pneumoniae*,[2] *Bacillus anthracis*,[3] and *Enterococcus faecium*.[4] In nature, the NAM–NAG bond is cleaved by a structurally diverse set of enzymes that can be classified using five prototypes derived from the >100 glycoside hydrolase families defined by CAZY[5] (recently reviewed in a historical context[6]): hen egg-white lysozyme (HEWL; GH22), goose egg-white lysozyme (GEWL, GH23), bacteriophage T4 lysozyme (T4L; GH24), *Sphingomonas* flagellar protein (FlgJ GH73),[7] and GH25 enzymes exemplified by *Chalaropsis* lysozymes.[8,9] The first three of these lysozyme types share some common structural features albeit with low sequence similarities. These GH22-24 enzymes consist mainly of a constant core of two helices and a three-stranded β-sheet that accommodates the substrates in the inter-domain cleft.[8] An additional family GH108 is likely to emerge as a sixth structural prototype,[9] although it remains largely biochemically uncharacterized. There are also several families of peptidoglycan lytic transglycosylases (reviewed by Blackburn and Clarke in Ref. 10) that will not be discussed further here.

The GH25 lysozymes, however, are structurally unrelated to the GH22-24, GH73, and GH108 lysozyme folds and instead these enzymes display a modified β-barrel-like fold that, like the classical 'TIM-barrel', is composed of a eight-stranded β-barrel, but which is flanked by five (as opposed to the normal eight) α-helices.[11] The characterized lysozymes from this family exhibit both β-1,4-*N*-acetyl- and β-1,4-*N*,6-*O*-diacetylmuramidase activities[12,13] and their evolutionary origin is diverse comprising bacterial, viral (mainly from phage), and eukaryotic representatives. So far three members of this family of enzymes have been structurally characterized, that of the *Streptomyces coelicolor* enzyme 'cellosyl',[11] the bacteriophage lysine PlyB,[14] and Clp-1 lysozyme from a *S. pneumoniae* phage[15,16] with the latter structure also obtained in complex with fragments of peptidoglycan analogues.[16]

* Corresponding author. Tel.: +44 1904 32 8278; fax: +44 1904 32 8266.
E-mail address: etaylor@ysbl.york.ac.uk (E.J. Taylor).

0008-6215/$ - see front matter © 2009 Elsevier Ltd. All rights reserved.
doi:10.1016/j.carres.2009.06.001

At the catalytic level, however, a serious drawback with mechanistic analysis of GH25 enzymes is the continuing lack of an appropriate substrate with which to determine the stereochemical course of hydrolysis given that, unlike hen egg-white lysozyme, for example, the enzymes are not active on NAG homopolymer 'chitooligosaccharide' substrates and have only been found to be active on the peptidoglycan found in intact bacterial cells. Thus, proposals as to mechanism have simply been inferred from the disposition of active center groups.[15] Briefly summarized, it is widely assumed that GH25 enzymes act with inversion of anomeric configuration which is a proposal based solely on the relative spacing of two conserved carboxylates in the enzyme active center that are deemed 'too distant' to be consistent with a classical retention mechanism via a covalent glycosyl-enzyme intermediate. Here we will argue, based upon our 1.4 Å crystal structure of a *B. anthracis* GH25 enzyme *Ba*GH25c (presented here for the first time) that these proposals are most likely incorrect. Whilst mechanistic clarification must await synthesis of a suitable substrate, we would propose, based upon the conserved active center similarity with hexosaminidases from families GH18, GH20, GH56, GH84, and GH85, that GH25 enzymes act, as with all these related families, with net retention of anomeric configuration. In the absence of any experimental evidence to the contrary, we suggest that GH25 enzymes harness a neighboring-group participation mechanism that has unambiguously been shown for the other enzyme families whose catalytic centers are highly similar to GH25.

Table 1
Data collection and refinement statistics

	*Ba*GH25c
Data processing	
Space group	$P6_122$
Unit cell lengths (Å)	$a = 100.5$, $b = 100.5$, $c = 106.7$
Unit cell angles (°)	$\alpha = \beta = 90$, $\gamma = 120$
Molecules in asymmetric unit	1
Resolution range (outer shell)	40.0–1.40 (1.48–1.40)
R_{merge}[a]	0.069 (0.432)
$\langle I/\sigma I \rangle$[a]	28.2 (5.1)
Completeness[a]	99.9 (100.0)
Redundancy[a]	16.3 (11.8)
Refinement statistics	
Resolution range (Å)	33.73–1.40
R_{cryst}	0.18
R_{free}	0.21
No. of protein atoms	2047
rmsd Bonds (Å)	0.016
rmsd Angles (°)	1.511
Mean B value of protein atoms (Å^2)	12
Mean B value of solvent atoms (Å^2)	28
ESU (Å^2)[b]	0.153
Ramachandran statistics[c]	98.7% Preferred regions, 1.3% allowed regions, 0.0% outliers
PDB code	2WAG

[a] Numbers in parentheses correspond to the high resolution outer shell.
[b] Estimated standard uncertainty, based upon R_{free}, calculated using REFMAC.
[c] Calculated using validation options in COOT.

2. Results and discussion

The gene encoding the *B. anthracis* GH25 enzyme, *Ba*GH25c, was expressed in *Escherichia coli*. The exact role of this protein in *B. anthracis* has not been described, but it is likely that this molecule modulates the chemical alteration of peptidoglycan during bacterial cell growth and division rather than being a prophage-encoded sequence. The gene is chromosomal, not adjacent to known prophage encoding genes and the protein sequence contains a signal secretion peptide—a feature not seen with phage-encoded lysins. The structure of *Ba*GH25c was solved by molecular replacement and was refined with diffraction data up to 1.4 Å resolution, Table 1. *Ba*GH25c crystallizes in space group $P6_122$ with one molecule in the asymmetric unit. The electron density map allowed tracing the entire chain of *Ba*GH25c from residue Met11 through to Met218 including the N-terminal His_6 tag, which was found to occlude the entrance of the catalytic crevice in the crystal form obtained. Despite much effort, we have been unable to find an alternative crystal form in the absence of the His-tag with which to embark on ligand-binding studies. The final model additionally comprises five sulfate ions, two glycerol molecules, five fragments of polyethylene glycol, and 372 water molecules.

The *Ba*GH25 sequences fold into a TIM barrel-like structure where the first five β-strands are flanked by α-helices and the last three strands are linked by loops without well-defined secondary structure equating to a $(\alpha/\beta)_5(\beta)_3$-barrel. The C-terminal β-strand runs anti-parallel to the rest of the β-strands closing the β-barrel through its interaction with the first N-terminal β-strand, Figure 1a. In agreement with sequence similarity comparisons, a structural search carried out with the SSM server[17] showed that the closest structural neighbors for *Ba*GH25C are members of the CAZy family GH25. Thus, the closest related structure is the bacterial lysozyme from *S. coelicolor* (Z-score 10.7, rmsd 1.5 Å over 195 Cα atoms) followed by PlyB, a bacteriophage-encoded lysin (Z-score 9.3, rmsd 1.74 Å over 167 Cα atoms) and CP-1, a cell wall endolysin from *S. pneumoniae* (Z-score 7.9, rmsd 2.0 Å over 164 Cα atoms). Despite relatively low sequence identities among the structurally characterized GH25 members (23–28%), a strong conservation is observed at the C-termini of the β-strands and this location corresponds to the entrance of the catalytic cavity. In *Ba*GH25c, as in the other GH25 members, this cavity is lined by a constellation of negatively charged and aromatic residues, Figure 1b.

Mutagenesis studies on the GH25 homologue CP-1[15,18] suggest that CP-1 Asp10 and Glu94 are the 'catalytic' carboxylates in this enzyme. In *Ba*GH25c, the equivalent residues are Asp20 and Glu107 which are found at the bottom of the catalytic crevice in a very similar position to that in the other known GH25 structures. *Ba*GH25c residue Asp20 forms a network of H-bonds to Gln184, Asp202, and Asn204; residues that appear strictly conserved in the GH25 family. Glu107, the other putative catalytic residue, is located about 8 Å away from Asp20 and interacts with Asp105, a residue which is also strictly conserved in the GH25 family. Superposition of the *Ba*GH25c coordinates onto the structure of the complex of Clp-1lysozyme with a peptidoglycan analogue shows no conservation around the residues that bind the sugar moieties in sub-sites +1 and +2 (Fig. 2; subsite nomenclature in Ref. 19). The loops surrounding these sites adopt different conformations in the two enzymes so in the absence of a complex structure the structural determinants that underlie the specificity of the *Ba*GH25c enzyme remain unknown. In the putative −1 site however, the structural equivalence is clear between the two enzymes and this conservation (shared with the rest of the structurally characterized GH25 enzymes) involves not only the presumed catalytic residues but also several aromatic residues that form a well-defined pocket whose entrance is about 7 Å wide and is 10 Å in depth.

As alluded to previously, the catalytic mechanism of GH25 enzymes has not been experimentally determined. It has been inferred from structural and mutagenesis data that GH25 enzymes operate with a classical inverting mechanism.[15,16] This is simply because of the spacing of the two 'catalytic' carboxylates which at 8–10 Å, are too far apart to suggest a retaining mechanism via a covalent glycosyl-enzyme intermediate[15] (the structural context of glycosidase mechanisms has historically[20] and more recently[21] been reviewed). It has therefore been assumed that the enzyme acts with inversion of anomeric configuration with Glu107 (*Ba*GH25c numbering) the catalytic acid and Asp20 acting as a catalytic base. Mutagenesis studies on the Clp-1 enzyme showed that

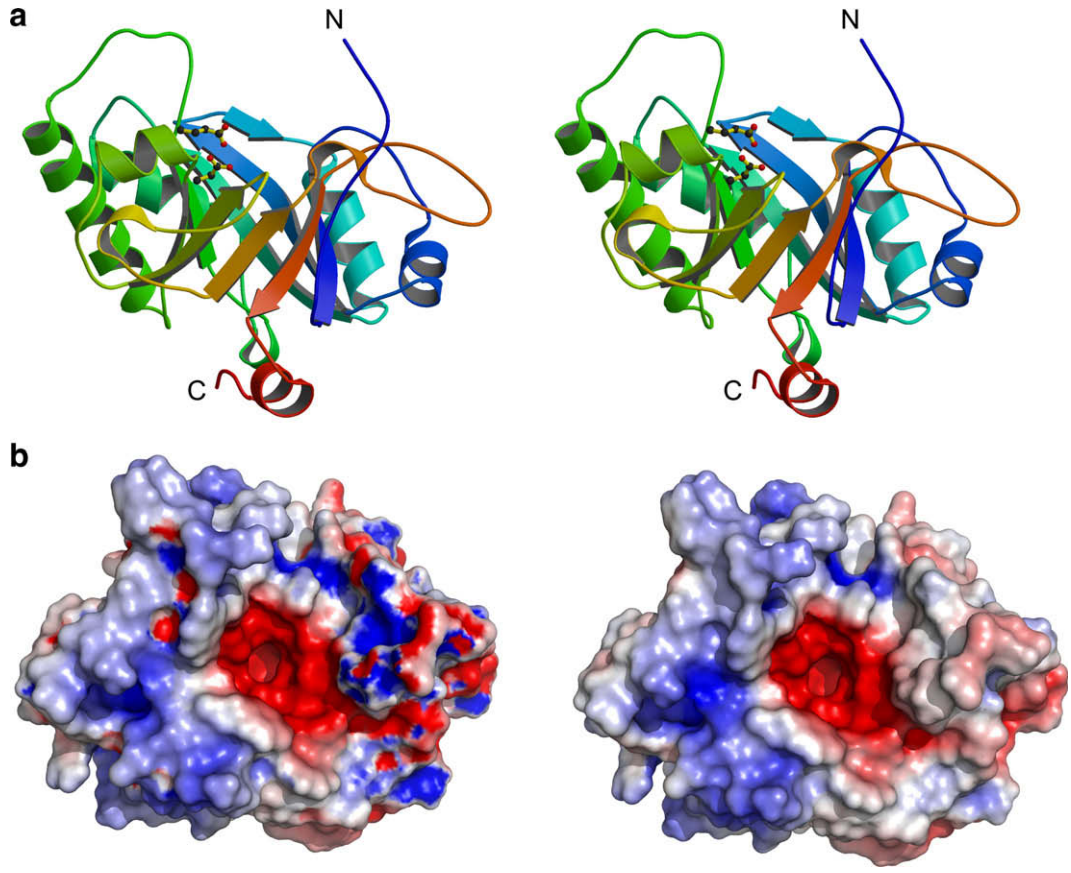

Figure 1. The 3-D structure of *Ba*GH25c. (a) Stereo color-ramped cartoon representation of the *Ba*GH25c fold with the potential catalytic pair shown in ball-and-stick and (b) stereo representation of the *Ba*GH25c electrostatic surface as calculated by APBS[44].

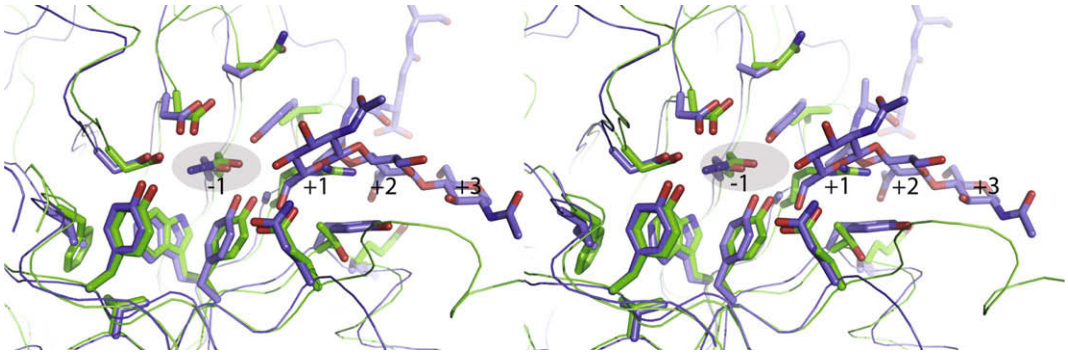

Figure 2. Wall-eyed stereo overlay of the active centers of *Ba*GH25c (green) and the complex of Cpl-1 with a peptidoglycan analogue (blue). Putative position of the −1 subsite is indicated with a gray oval.

Glu94 (BaGH25c Glu107) is an important residue for activity since the Gln or Ala variants at this position reduce the activity more than 10^4-fold relative to the wild-type enzyme. The proposed base in the implied inverting mechanism was Asp10, with the Asp10Ala variant resulting in a protein that retained about 0.2% activity relative to the wild-type enzyme.[18] This residual activity is somewhat difficult to reconcile with equivalent variants in inverting enzymes where the reduction in activity is usually greater than 10^5 fold (see e.g.,[22]). This situation leaves the GH25 mechanism still open to question.

It is our view that the assumption of an inverting mechanism simply because of a spacing of two carboxylates >5.5 Å is incorrect. We observe that the structure of the catalytic cavity of BaGH25c carries a striking resemblance to the catalytic centers of enzymes from families GH18,[23] GH20,[24] GH56,[25] GH84,[26] and GH85,[27,28] Figure 3. All of these β-*N*-acetylglucosamidases act on similar substrates using a substrate-assisted or 'neighboring group' catalytic mechanism with net retention of anomeric configuration; a mechanism that has been intensely studied on various systems (e.g.,[29–33]). Additionally, the $(\alpha/\beta)_8$-barrel topologies of these enzymes share much with the modified $(\alpha/\beta)_5(\beta)_3$-barrel of the GH25 enzymes with a common active center at the entrance of the β-barrel opening. The pockets formed at this location are lined by several aromatic residues that accommodate the substrate while the catalytic residues, usually a pair of carboxylate residues close in primary structure, are placed with the general acid/base catalyst located above the sugar ring.

The neighboring-group mechanism, as witnessed in GH18, GH20, GH56, GH84, and GH85, consists of a double displacement

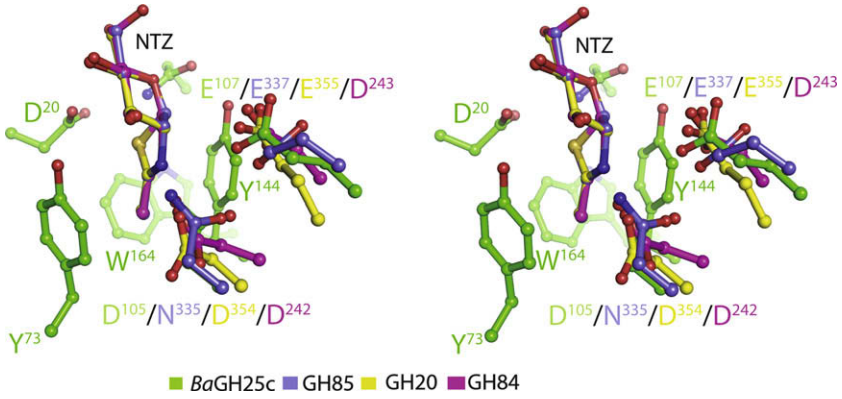

Figure 3. Stereo representation of the superposition of the catalytic cavities of GH20 (yellow, PDB code 1NP0), GH84 (purple, PDB code 2CHN), GH85 (blue, PDB code 2W92), and BaGH25c (green) around the coordinates of their NAG–thiazoline complexes.

mechanism in which the nucleophile is not derived from the enzyme but instead is from the intramolecular 'neighboring group' attack of the *N*-acetyl carbonyl group.[21] Thus catalysis occurs via the formation, and subsequent breakdown of a covalent oxazoline intermediate, Figure 4. In the above-mentioned families, there is a classical signature constellation of catalytic apparatus, twin carboxylate-bearing side chains either adjacent or separated by a single residue, in the primary sequence. One of these residues acts as the catalytic acid/base, initially protonating the leaving group to facilitate its departure (general acid assistance) and subsequently acting as a general base to activate the hydrolytic water molecule. The second residue (normally Asp or Glu), but Asn in the unusual GH85 enzymes[28,31] acts to stabilize or deprotonate the oxazoline nitrogen, Figure 4.

This signature motif is seen in all GH25 enzymes studied with the residues lying exactly as seen in GH18, GH20, GH56, GH84, and GH85 which must also strongly support a mechanism with retention of anomeric configuration for GH25 enzymes. When representatives of these classes of enzymes are superposed with BaGH25c around the coordinates of their respective complexes with a potent inhibitor of neighboring-group participating enzymes NAG–thiazoline, it is apparent that the GH25 enzyme shares the active site topology from which we suggest that the catalytic residues are in the *Ba*GH25c enzyme the carboxylate pair Asp105 and Glu107, residues that together with several of the aromatic side chains lining the pocket are strictly conserved across the GH25 family. Additionally, we observed in this superposition that the role of the Cpl-1 Asp10 (BaGH25c Asp20) is not necessarily related to catalysis but may be only involved in substrate recognition which may explain the residual activity of its Ala variant referred to above. We therefore conclude that until experimental data on the stereochemistry of GH25 hydrolysis of peptidoglycan have been achieved, following the synthesis or isolation of an appropriate soluble substrate, the absolute conservation of the classical neighboring-group participation motifs in the 3-D structure strongly suggests a mechanism with retention of anomeric configuration via an oxazoline intermediate. Given that mimicry of the oxazoline and its closely related transition states is a validated route into potential therapeutic agents (e.g.,[34]) this mechanistic re-evaluation may lead to chemical tools with which to probe bacterial pathogenicity in future.

3. Experimental

3.1. Cloning, expression, and purification of the BaGH25c

The Ba*GH25c* gene (UniProt:Q81YN8) was amplified by PCR from *B. anthracis* str. Ames[35] genomic DNA using the forward primer CACCACCACCACAT GGATAGGTATGAAATAAAAGGTGTAGAT and reverse primer GAGGAGAAGGCGCGTTAATCTTTCATTCCATAATTCTCA AACTCTTCCT CATTC. The gene was then cloned into pET28a for expression purposes with an N-terminal His_6 tag. The expression construct was transformed into BL21(DE3) cells and cultures were grown at 37 °C until $O.D._{600}$ of 0.4. The incubation temperature was then decreased to 30 °C prior to induction with IPTG overnight. *Ba*GH25c was purified from cell-free extracts via Ni-affinity chromatography followed by gel filtration. Pure protein as judged by SDS–PAGE was concentrated between 4 and 5 mg/mL and buffer exchanged into 20 mM HEPES pH 7.2 using a Vivaspin 10-kDa cut-off concentrator prior to crystallization.

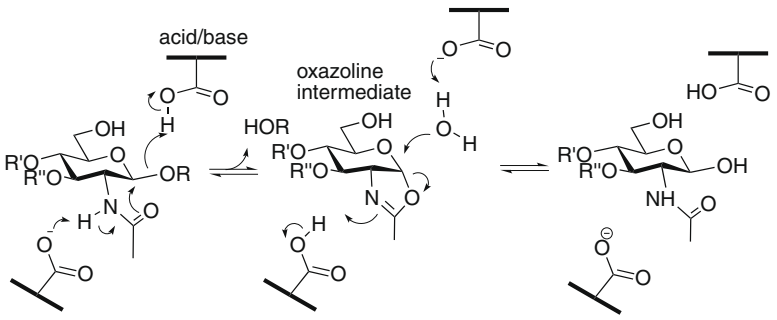

Figure 4. Reaction mechanism for glycoside hydrolysis, using a neighboring-group catalytic mechanism via a covalent oxazoline intermediate, leading to net retention of anomeric configuration. The active center of GH25 enzymes is fully consistent with this mechanism shared with enzymes from GH18, GH20, GH56, GH84, and GH85. R is any leaving group, R′ = H (in the case of an *exo*-acting enzyme (GH20, GH84), or the appropriate poly/oligosaccharide chain in the case of an *endo*-acting enzyme such as GH18 chitinases, GH25 lysins, GH56 hyaluronidases, or GH85 *endo* β-*N*-acetylglucosaminidases. R″ = H (*N*-acetyl glucosamine-based substrates) or a lactyl group (=$CHCH_3COOH$) in *N*-acetylmuramic acid).

3.2. Crystallization and structure solution

The *Ba*GH25c protein was screened in 300 nL drops using a mosquito robot together with the Hampton Crystal screen, Crystal screen 2, and Hampton PEG/Ion screen (Hampton research, Alison Viejo, CA). Conditions were optimized using the hanging drop vapor diffusion method. Drops containing 1 μL of protein were mixed together with 2 μL of the mother liquor. Initial crystals were found to grow in Hampton Crystal screen condition A4. This condition was further optimized to improve crystal quality resulting in final condition that consisted of 2.1 M $(NH_4)_2SO_4$ and 0.1 M Tris–HCl pH 8.5. A cryoprotectant solution was produced by supplementing the mother liquor with 25% (v/v) glycerol. Crystals were harvested in rayon fiber loops, bathed in cryoprotectant solution prior to flash freezing in liquid nitrogen.

Diffraction data were collected on the European Synchrotron Radiation Facility (ESRF) from single crystals at 100 K with an oscillation range of 0.5°. Data were collected at a wavelength of 0.933 Å on beamline ID14-2 using an ADSC Q4R CCD detector. All diffraction data were processed with MOSFLM and reduced and scaled with SCALA.[36] All other computing was undertaken using the CCP4 suite[37] unless otherwise specified. The structure of *Ba*GH25c was solved by molecular replacement using the program AMORE[38] using the *S. coelicolor* lysozyme structure[11] (PDB code 1JFX) as a search model. 5% of the total reflections were set aside for cross-validation ('R_{free}') purposes and for the weighting of geometrical and temperature factor restraints. Automatic model building was carried out with ARP/wARP[39] interspaced with refinement cycles that used REFMAC.[40] Solvent molecules were added using COOT[41] and checked manually. The structure was validated using MOLPROBITY[42] prior to deposition. The structure and observed structure factors are accessible with PDB code 2WAG. Data collection and refinement statistics are given in Table 1. Structure figures were drawn with PYMOL (DeLano Scientific www.pymol.org) and MOLSCRIPT.[43]

Acknowledgments

We gratefully acknowledge the financial support from the Royal Society and the Biotechnology and Biological Sciences Research Council (BBSRC). EJT is a Royal Society-University Research Fellow and GJD is a Royal Society-Wolfson Research Merit Award recipient.

References

1. Nelson, D.; Loomis, L.; Fischetti, V. A. *Proc. Natl. Acad. Sci. U.S.A.* **2001**, *98*, 4107–4112.
2. Loeffler, J. M.; Djurkovic, S.; Fischetti, V. A. *Infect Immun.* **2003**, *71*, 6199–6204.
3. Schuch, R.; Nelson, D.; Fischetti, V. A. *Nature* **2002**, *418*, 884–889.
4. Yoong, P.; Schuch, R.; Nelson, D.; Fischetti, V. A. *J. Bacteriol.* **2004**, *186*, 4808–4812.
5. Cantarel, B. L.; Coutinho, P. M.; Rancurel, C.; Bernard, T.; Lombard, V.; Henrissat, B. *Nucleic Acids Res.* **2008**, *37*, D233–238.
6. Davies, G. J.; Sinnott, M. L. *Biochem. J.* **2008**. doi:10.1042/BJ20080382 (online only).
7. Hashimoto, W.; Ochiai, A.; Momma, K.; Itoh, T.; Mikami, B.; Maruyama, Y.; Murata, K. *Biochem. Biophys. Res. Commun.* **2009**, *381*, 16–21.
8. Monzingo, A. F.; Marcotte, E. M.; Hart, P. J.; Robertus, J. D. *Nat. Struct. Biol.* **1996**, *3*, 133–140.
9. Stojkovic, E. A.; Rothman-Denes, L. B. *J. Mol. Biol.* **2007**, *366*, 406–419.
10. Blackburn, N. T.; Clarke, A. J. *J. Mol. Evol.* **2001**, *52*, 78–84.
11. Rau, A.; Hogg, T.; Marquardt, R.; Hilgenfeld, R. *J. Biol. Chem.* **2001**, *276*, 31994–31999.
12. Vollmer, W.; Joris, B.; Charlier, P.; Foster, S. *FEMS Microbiol. Rev.* **2008**, *32*, 259–286.
13. Fouche, P. B.; Hash, J. H. *J. Biol. Chem.* **1978**, *253*, 6787–6793.
14. Porter, C. J.; Schuch, R.; Pelzek, A. J.; Buckle, A. M.; McGowan, S.; Wilce, M. C.; Rossjohn, J.; Russell, R.; Nelson, D.; Fischetti, V. A.; Whisstock, J. C. *J. Mol. Biol.* **2007**, *366*, 540–550.
15. Hermoso, J. A.; Monterroso, B.; Albert, A.; Galan, B.; Ahrazem, O.; Garcia, P.; Martinez-Ripoll, M.; Garcia, J. L.; Menendez, M. *Structure* **2003**, *11*, 1239–1249.
16. Perez-Dorado, I.; Campillo, N. E.; Monterroso, B.; Hesek, D.; Lee, M.; Paez, J. A.; Garcia, P.; Martinez-Ripoll, M.; Garcia, J. L.; Mobashery, S.; Menendez, M.; Hermoso, J. A. *J. Biol. Chem.* **2007**, *282*, 24990–24999.
17. Krissinel, E.; Henrick, K. *Acta Crystallogr., Sect. D* **2004**, *60*, 2256–2268.
18. Sanz, J. M.; Garcia, P.; Garcia, J. L. *Biochemistry* **1992**, *31*, 8495–8499.
19. Davies, G. J.; Wilson, K. S.; Henrissat, B. *Biochem. J.* **1997**, *321*, 557–559.
20. Davies, G.; Henrissat, B. *Structure* **1995**, *3*, 853–859.
21. Vocadlo, D.; Davies, G. J. *Curr. Opin. Chem. Biol.* **2008**, *12*, 539–555.
22. Nurizzo, D.; Turkenburg, J. P.; Charnock, S. J.; Roberts, S. M.; Dodson, E. J.; McKie, V. A.; Taylor, E. J.; Gilbert, H. J.; Davies, G. J. *Nat. Struct. Biol.* **2002**, *9*, 665–668.
23. Terwisscha Van Scheltinga, A. C.; Armand, S.; Kalk, K. H.; Isogai, A.; Henrissat, B.; Dijkstra, B. W. *Biochemistry* **1995**, *34*, 15619–15623.
24. Tews, I.; Perrakis, A.; Oppenheim, A.; Dauter, Z.; Wilson, K. S.; Vorgias, C. E. *Nat. Struct. Biol.* **1996**, *3*, 638–648.
25. Markovic-Housley, Z.; Miglierini, G.; Soldatova, L.; Rizkallah, P. J.; Muller, U.; Schirmer, T. *Structure* **2000**, *8*, 1025–1035.
26. Dennis, R. J.; Taylor, E. J.; Macauley, M. S.; Stubbs, K. A.; Turkenburg, J. P.; Hart, S. J.; Black, G.; Vocadlo, D. J.; Davies, G. J. *Nat. Struct. Mol. Biol.* **2006**, *13*, 365–371.
27. Abbott, D. W.; Macauley, M. S.; Vocadlo, D. J.; Boraston, A. B. *J. Biol. Chem.* **2009**, *284*, 11676–11689.
28. Ling, Z.; Suits, M. D.; Bingham, R. J.; Bruce, N. C.; Davies, G. J.; Fairbanks, A. J.; Moir, J. W.; Taylor, E. J. *J. Mol. Biol.* **2009**, *389*, 1–9.
29. Drouillard, S.; Armand, S.; Davies, G. J.; Vorgias, C. E.; Henrissat, B. *Biochem. J.* **1997**, *328*, 945–949.
30. Macauley, M. S.; Whitworth, G. E.; Debowski, A. W.; Chin, D.; Vocadlo, D. J. *J. Biol. Chem.* **2005**, *280*, 25313–25322.
31. Abbott, D. W.; Macauley, M. S.; Vocadlo, D. J.; Boraston, A. B. *J. Biol. Chem.* **2009**.
32. Macauley, M. S.; Stubbs, K. A.; Vocadlo, D. J. *J. Am. Chem. Soc.* **2005**, *127*, 17202–17203.
33. Mark, B. L.; Vocadlo, D. J.; Zhao, D.; Knapp, S.; Withers, S. G.; James, M. N. *J. Biol. Chem.* **2001**, *276*, 42131–42137.
34. Yuzwa, S. A.; Macauley, M. S.; Heinonen, J. E.; Shan, X. Y.; Dennis, R. J.; He, Y. A.; Whitworth, G. E.; Stubbs, K. A.; McEachern, E. J.; Davies, G. J.; Vocadlo, D. J. *Nat. Chem. Biol.* **2008**, *4*, 483–490.
35. Read, T. D.; Peterson, S. N.; Tourasse, N.; Baillie, L. W.; Paulsen, I. T.; Nelson, K. E.; Tettelin, H.; Fouts, D. E.; Eisen, J. A.; Gill, S. R.; Holtzapple, E. K.; Okstad, O. A.; Helgason, E.; Rilstone, J.; Wu, M.; Kolonay, J. F.; Beanan, M. J.; Dodson, R. J.; Brinkac, L. M.; Gwinn, M.; DeBoy, R. T.; Madpu, R.; Daugherty, S. C.; Durkin, A. S.; Haft, D. H.; Nelson, W. C.; Peterson, J. D.; Pop, M.; Khouri, H. M.; Radune, D.; Benton, J. L.; Mahamoud, Y.; Jiang, L.; Hance, I. R.; Weidman, J. F.; Berry, K. J.; Plaut, R. D.; Wolf, A. M.; Watkins, K. L.; Nierman, W. C.; Hazen, A.; Cline, R.; Redmond, C.; Thwaite, J. E.; White, O.; Salzberg, S. L.; Thomason, B.; Friedlander, A. M.; Koehler, T. M.; Hanna, P. C.; Kolsto, A. B.; Fraser, C. M. *Nature* **2003**, *423*, 81–86.
36. Leslie, A. G. W. (1992). Recent changes to the MOSFLM package for processing film and image plate data. *Joint CCP4 and ESF-EACMB newsletter on protein crystallography*: Daresbury Laboratory, Warrington, UK.
37. Collaborative Computational Project Number 4. *Acta Crystallogr., Sect. D* **1994**, *50*, 760–763.
38. Navaza, J. *Acta Crystallogr., Sect. D* **2001**, *57*, 1367–1372.
39. Perrakis, A.; Harkiolaki, M.; Wilson, K. S.; Lamzin, V. S. *Acta Crystallogr., Sect. D* **2001**, *57*, 1445–1450.
40. Murshudov, G. N.; Vagin, A. A.; Dodson, E. J. *Acta Crystallogr., Sect. D* **1997**, *53*, 240–255.
41. Emsley, P.; Cowtan, K. *Acta Crystallogr., Sect. D* **2004**, *60*, 2126–2132.
42. Davis, I. W.; Leaver-Fay, A.; Chen, V. B.; Block, J. N.; Kapral, G. J.; Wang, X.; Murray, L. W.; Arendall, W. B., 3rd; Snoeyink, J.; Richardson, J. S.; Richardson, D. C. *Nucleic Acids Res.* **2007**, *35*, W375–383.
43. Kraulis, P. J. *J. Appl. Crystallogr.* **1991**, *24*, 946–950.
44. Baker, N. A. *Methods Enzymol.* **2004**, *383*, 94–118.